
Article:
Ofman, Tim P., Heming, Jurriaan J. A., Nin-Hill, Alba et al. (15 more authors) (2024) Conformational and Electronic Variations in 1,2- and 1,6-Cyclophellitols and Their Impact on Retaining α-Glucosidase Inhibition. Chemistry - A European Journal. ISSN: 0947-6539

https://doi.org/10.1002/chem.202400723

Chemistry–A European Journal
Research Article
doi.org/10.1002/chem.202400723
Chemistry Europe
European Chemical Societies Publishing
www.chemeurj.org

Conformational and Electronic Variations in 1,2- and 1,5a-Cyclophellitols and their Impact on Retaining α-Glucosidase Inhibition

Tim P. Ofman,[a] Jurriaan J. A. Heming,[a] Alba Nin-Hill,[b] Florian Küllmer,[a] Elisha Moran,[c] Megan Bennett,[c] Roy Steneker,[a] Anne-Mei Klein,[a] Gijs Ruijgrok,[a] Ken Kok,[a] Zach W. B. Armstrong,[c] Johannes M. F. G. Aerts,[a] Gijsbert A. van der Marel,[a] Carme Rovira,[b, d] Gideon J. Davies,[c] Marta Artola,[a] Jeroen D. C. Codée,[a] and Herman S. Overkleeft*[a]

Glycoside hydrolases (glycosidases) take part in myriad biological processes and are important therapeutic targets. Competitive and mechanism-based inhibitors are useful tools to dissect their biological role and comprise a good starting point for drug discovery. The natural product, cyclophellitol, a mechanism-based, covalent and irreversible retaining β-glucosidase inhibitor has inspired the design of diverse α- and β-glycosidase inhibitor and activity-based probe scaffolds. Here, we sought to deepen our understanding of the structural and functional requirements of cyclophellitol-type compounds for effective human α-glucosidase inhibition. We synthesized a comprehensive set of α-configured 1,2- and 1,5a-cyclophellitol analogues bearing a variety of electrophilic traps. The inhibitory potency of these compounds was assessed towards both lysosomal and ER retaining α-glucosidases. These studies revealed the 1,5a-cyclophellitols to be the most potent retaining α-glucosidase inhibitors, with the nature of the electrophile determining inhibitory mode of action (covalent or non-covalent). DFT calculations support the ability of the 1,5a-cyclophellitols, but not the 1,2-congeners, to adopt conformations that mimic either the Michaelis complex or transition state of α-glucosidases.

Introduction

Carbohydrates are found abundantly in nature and are essential in numerous biological processes.[1–4] The vast structural variation found in glycans is evident in the large variety of hydrolytic enzymes that have emerged and that are responsible for their processing and degradation. This large family of glycoside hydrolases is categorized in over 180 subfamilies, based on their primary sequence, tertiary structure and function (www.cazy.org).[5] Understanding their mode of action is an important step in the rational design of compounds that can selectively and efficiently inhibit specific glycoside hydrolases. Retaining glycoside hydrolases, which comprise a large part of the known glycosidases, encompass the human GH31 retaining α-glucosidases subject of the here-presented studies. Retaining α-glucosidases classically employ a Koshland double displacement mechanism (Figure 1A).[6] Typically, two carboxylic acid residues residing in the enzyme active site are positioned in such a way that one residue can act as a nucleophile and the other as a catalytic acid/base. Upon binding of the substrate in the active site, a Michaelis complex is formed with the substrate (in general the case of retaining α-glucosidases) adopting a $^4C_1$-conformation. In this way, the leaving group is positioned axially, allowing protonation by the catalytic acid-base and subsequent nucleophilic displacement of the aglycon by the nucleophilic acid residue. This process proceeds through a glucosyl $^4H_3$ oxocarbenium ion-like transition state and results in the formation of a covalent intermediate, with the bound glucose adopting a $^1S_3$-conformation. Next and following the expulsion of the aglycon, water enters the active site. Following a reversed conformational itinerary ($^1S_3 \rightarrow {}^4H_3 \rightarrow {}^4C_1$), α-glucose is released and the enzyme returned to its resting phase ready for another catalytic cycle.[7–11] Knowledge of these conformational itineraries allows both the interpretation and design of potent

[a] Dr. T. P. Ofman, J. J. A. Heming, Dr. F. Küllmer, R. Steneker, A.-M. Klein, G. Ruijgrok, K. Kok, Prof. Dr. J. M. F. G. Aerts, Prof. Dr. G. A. van der Marel, Dr. M. Artola, Prof. Dr. J. D. C. Codée, Prof. Dr. H. S. Overkleeft
Leiden Institute of Chemistry, Leiden University
Einsteinweg 55, 2333 CC Leiden, The Netherlands
E-mail: h.s.overkleeft@chem.leidenuniv.nl

[b] Dr. A. Nin-Hill, Prof. Dr. C. Rovira
Departament de Química Inorgànica i Orgànica (Secció de Química Orgànica) and Institut de Química Teòrica i Computacional (IQTCUB)
Universitat de Barcelona
Martí i Franques 1–11, E-08028 Barcelona, Spain

[c] E. Moran, M. Bennett, Dr. Z. W. B. Armstrong, Prof. Dr. G. J. Davies
York Structural Biology Laboratory, Department of Chemistry
University of York
Heslington YO10 5DD, United Kingdom

[d] Prof. Dr. C. Rovira
Institució Catalana de Recerca i Estudis Avançats (ICREA)
08020 Barcelona (Spain)

Supporting information for this article is available on the WWW under https://doi.org/10.1002/chem.202400723

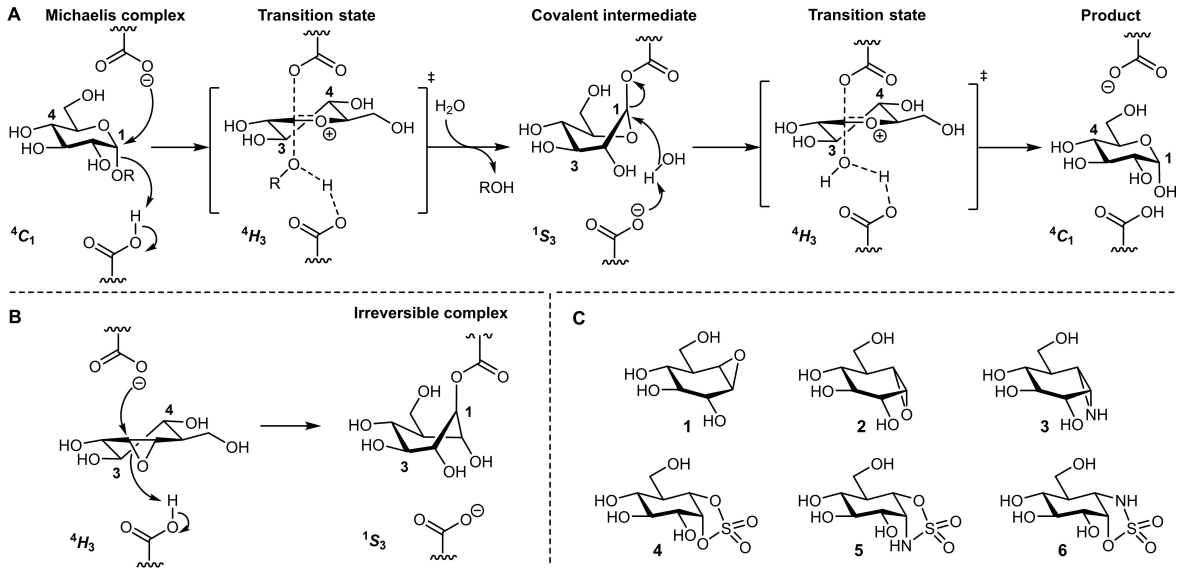

Figure 1. (A) Mechanistic itinerary of retaining α-glucosidases, (B) mechanism of inhibition by 1,5a-*epi*-cyclophellitol **2** and (C) a selection of established covalent and non-covalent inhibitors of retaining β-glucosidases (**1**) and α-glucosidases (**2**–**6**).

inhibitors and activity-based probes, such as those based on cyclophellitol, as described here.

Cyclophellitol (**1**), a natural product found in the *Phellinus sp.* mushroom, is a potent mechanism-based, covalent and irreversible retaining β-glucosidase inhibitor.[12] Cyclophellitol is the carbocyclic analogue of natural retaining β-glucosidase substrates (β-glucopyranosides), bearing an epoxide bridging the C1 and C5a position (IUPAC numbering).[13–15] This epoxide also effectively constrains the cyclohexane into a $^4H_3$ conformation thereby mimicking the transition state (TS) during hydrolysis of β-glucopyranoses by retaining β-glucosidases. Not long after the discovery of cyclophellitol and fuelled by its rare mode of action, the 1,5a-epimer of cyclophellitol was synthesized and shown to be a mechanism-based inhibitor of retaining α-glucosidases.[16]

Upon binding of 1,5a-*epi*-cyclophellitol (**2**) to the active site of a retaining α-glucosidase, the nucleophilic carboxylate opens the (protonated) epoxide in a *trans*-diaxial fashion forming an irreversible, covalent ester linkage with the inhibitor, thereby incapacitating the enzyme (Figure 1B). This *modus operandi* has been well-appreciated in the design of activity-based protein profiling (ABPP) as tools in chemical glycobiology.[17–21] Previously, we have shown 1,5a-*epi*-cyclophellitol (**2**) and its nitrogen congener (**3**) to be effective irreversible inhibitors with micromolar to nanomolar affinities for human acid α-glucosidase (GAA) and endoplasmic reticulum glucosidase II (ER-II, Figure 1C).[20,22] Notably, given the occasional off-target effects of 1,5a-*epi*-cyclophellitol, replacing the epoxide by a cyclic sulfate (as in **4**) resulted in an inhibitor with excellent potency and selectivity for α-glucosidases.[23] Conformationally, compound **4** does not exhibit $^4H_3$ character since the ring is not distorted by a strained three-membered ring. Rather, a $^4C_1$ conformation is adopted mimicking the structure of the α-glucosyl substrate in the Michaelis complex instead. As a follow up study and with the aim to reduce the electrophilicity of the cyclic sulfate, the corresponding cyclic sulfamidates (**5** and **6**) were developed as retaining α-glucosidase inhibitors.[24] Due to the non-covalent binding mode of compound **5**, this ligand was further evaluated as enzyme stabilizer and pharmacological chaperone for the possible treatment of Pompe disease, in which the lysosomal α-glucosidase GAA is genetically impaired.[25–27] Altogether, these results invite for a more in-depth study of modified cyclophellitol analogues as mechanism-based inhibitors.

Here, the synthesis and inhibitory potential of α-1,2-cyclophellitol (**12**–**21**, Figure 2) in comparison with α-1,5a-*epi*-cyclophellitols (**2**–**11**) is described. The inhibitory potencies and mode of action of the focused library of cyclophellitols on GAA and ER-II was studied in comparison to their parent compound, α-1,5a-*epi*-cyclophellitol (**2**). Some compounds proved to be more potent than lead structure (**2**), with low micromolar inhibition constants (IC_{50}) observed for these. In all, the work presented here comprises expansion of the cyclophellitol scaffold in the design of both covalent and competitive retaining glycosidase inhibitors, including chemistries that can be readily adapted to differently configured carbohydrate mimetics and that would target glycosidases other than the α-glucosidase ones studied here.

Results and Discussion

Compound synthesis. Compound **22** (Scheme 1), the key intermediate from which all 1,2-cyclophellitols were derived, was synthesized in eight steps according to procedures of Crotti *et al.* and Nagarajan *et al.* (See SI, Scheme S1).[28,29] Epoxidation of the double bond in **22** under the *aegis* of *m*-CPBA yielded a separable mixture of epoxides **23** and **24** in 53% and 26% yield, respectively.

Reductive deprotection (Pd/C, H_2) of α-epoxide **23** yielded **12** (83%) as the first target compound, of which all spectro-

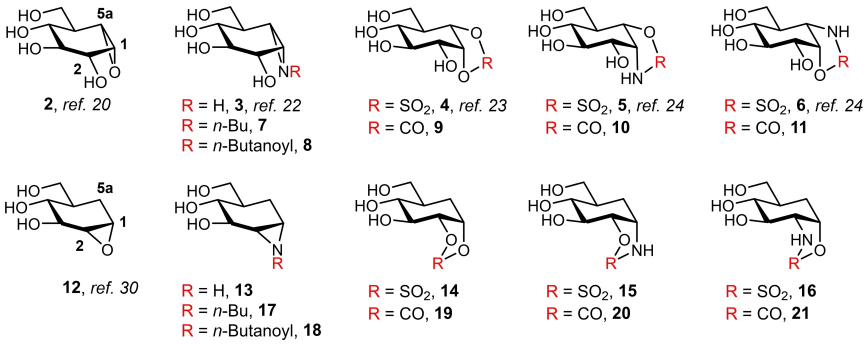

Figure 2. Twenty cyclophellitol analogues studied in this paper for their inhibitory activity against human retaining α-glucosidases.

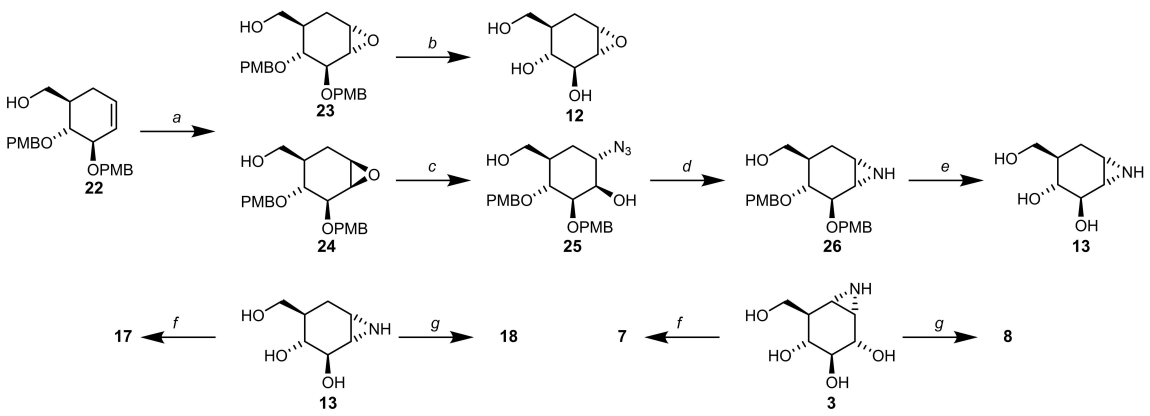

Scheme 1. Synthesis of compounds **7**, **8**, **12**, **13**, **17** and **18**. Reagents and conditions: (a) *m*-CPBA, DCM, 18 h, rt, 53% (**23**), 26% (**24**); (b) Pd/C, H_2, MeOH, 1 h, rt (83%); (c) NaN_3, DMF, 18 h, 130 °C (60%); (d) TPP, CH_3CN, 18 h, 60 °C (43%); (e) Na, NH_3, 1 h, −60 °C (92%); (f) butyl iodide, K_2CO_3, DMF, 18 h, 80 °C, 84% (**17**), 24% (**7**); (g) butanoyl chloride, Et_3N, MeOH, 30 min, 0 °C, 50% (**18**), 64% (**8**).

scopic data were in full agreement with those reported in literature.[30] Following established procedures, [31] opening of the β-epoxide with sodium azide under elevated temperatures yielded **25** (60%) which was subsequently treated with triphenylphosphine to undergo an intramolecular Staudinger cyclisation to yield α-aziridine **26** as the single regioisomer (43%). Removal of the 4-methoxybenzyl protecting groups in **26** was accomplished using Birch conditions (Na, NH_3) yielding target compound **13** (92%). Treatment of the α-aziridine with either butyl iodide or butanoyl chloride yielded the butylated aziridine **17** and butanoylated aziridine **18** in 84% and 50% respectively. The butylated and butanoylated 1,5a-α-aziridines (**7** and **8**) were obtained *via* identical conditions starting from 1,5a-α-aziridine **3**, which was in turn synthesized according to procedures optimized as published previously.[22,32] Cyclic sulfate **14** and carbonate **19** were constructed starting with protection of the primary hydroxyl in **22** as the 4-methoxybenzyl ether under Williamson etherification conditions (NaH, PMBCl) to yield compound **27** in 85% (Scheme 2). Subsequent dihydroxylation of the alkene ($RuCl_3$, $NaIO_4$) yielded solely α-*cis*-diol **28** (85%)

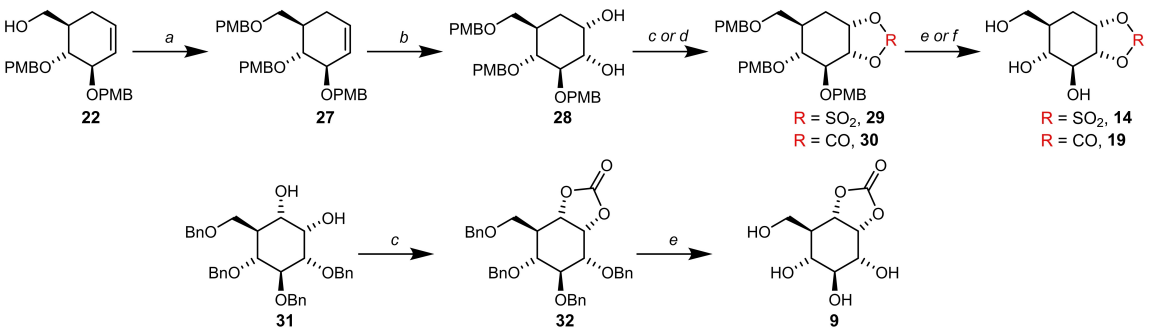

Scheme 2. Synthesis of **9**, **14** and **19**. Reagents and conditions: (a) PMBCl, NaH, DMF, 16 h, rt (85%); (b) $RuCl_3$, $NaIO_4$, 1:4:4 H_2O:CH_3CN:EtOAc, 1 h, 0 °C (85%); (c) triphosgene, pyridine, DCM, 1.5 h, rt, 86% (**30**), 90% (**32**); (d) (i) $SOCl_2$, Et_3N, DCM, 1 h, rt; (ii) $RuCl_3$, $NaIO_4$, 1:1 H_2O:CH_3CN, 15 min, 0 °C, 46% (**29**); (e) $Pd(OH)_2$/C, H_2, MeOH, 18 h, rt, 68% (**19**), quant. (**9**); (f) Pd/C, H_2, MeOH, 18 h, rt, 83% (**14**).

which was either sulfurylated ($SOCl_2$, Et_3N, *then* $RuCl_3$, $NaIO_4$) or carbonylated (triphosgene, Et_3N) to yield cyclic sulfate **29** (46%) and cyclic carbonate **30** (86%) respectively. Hydrogenation yielded the final compounds **14** and **19** in 83% and 68% respectively. In addition, 1,5a-α-carbonate **9** was obtained *via* identical conditions starting from 1,5a-α-*cis*-diol **31**, which was in turn synthesized according to procedures published previously.[23] Cyclic sulfamidates **15** and **16** and carbamates **20** and **21** were constructed *via* a stereoselective Sharpless amino-hydroxylation on alkene **27** ($K_2[OsO_2(OH)_4]$, chloramine-T, TEBACl) to give a separable, regioisomeric mixture of α-*cis*-amino alcohols **33** and **34** in 54% and 31% respectively (Scheme 3).[33] Both α-*cis*-amino alcohols could be transformed into their corresponding cyclic sulfamidates by treatment with sulfuryl chloride and Et_3N at low temperatures (−78 °C) in quantitative yields. Subsequent removal of the *N*-tosyl functionality under reductive conditions (Na, naphthalene) gave rise to cyclic sulfamidates **35** and **37** in 75% and 85% yield respectively. Alternatively, treatment of the individual amino alcohols **33** and **34** with triphosgene and pyridine followed by subsequent reductive detosylation (Na, naphthalene) yielded cyclic carbamates **36** and **38** (71% and 79% respectively, yield over two steps). Global deprotection with TFA and triethylsilane as cation scavenger afforded target sulfamidates **15** and **16** and carbamates **20** and **21** in 94%, 81%, 67% and 32% respectively.

Cyclic carbamates **10** and **11** were constructed *via* global deprotection of intermediates **40** and **41** (Scheme 4). Compounds **40** and **41** were synthesized from parent structure **39**,[34–36] according to modified literature procedures (See SI, Scheme S2).[24] A two-step deprotection sequence then proceeded smoothly by Apparent IC_{50} values were determined by measuring hydrolysis of the fluorogenic substrate, 4-methylulbelliferyl-α-D-glucose, where release of fluorescent product (4-methylumbelliferonate) is determined in terms of relative absorption (see SI). Epoxide **12** proved to be a micromolar inhibitor of rhGAA treating compounds **40** and **41** with a Brønsted acid (*p*-TsOH, MeOH) followed by treating the purified intermediates (S18 and S19) with TFA and triethylsilane. This afforded the target structures **10** and **11** in moderate to good yield (74% and 86% respectively).

***In vitro* inhibition of human acid α-glucosidase and ER α-glucosidase II.** With inhibitors **2–21** in hand, attention was turned to evaluating their inhibitory potencies as inhibitors against recombinant human acid α-glucosidase (rhGAA) and ER α-glucosidase II (ER-II, Table 1). Although inhibition by covalent inhibitors reflects both initial binding and subsequent covalent rate (see below), IC_{50} measurements provide a facile initial way to compare inhibitory potency.

($IC_{50} = 32.4 \pm 4.6$ μM) making it slightly less potent than its 1,5a-counterpart **2** ($IC_{50} = 6.7 \pm 0.34$ μM).[23] In contrast, superior inhibitory potency was observed for **12** ($IC_{50} = 11.3 \pm 0.5$ μM) when screened against ER-II. Aziridine **13** showed to be inactive on rhGAA, while inhibiting ER-II in the micromolar range ($IC_{50} = 46.2 \pm 2.6$ μM), whilst its 1,5a-counterpart **3** tested to be a sub-micromolar inhibitor of both rhGAA ($IC_{50} = 0.34 \pm 0.091$ μM) and ER-II ($IC_{50} = 1.5 \pm 0.08$ μM).[23] *n*-Butyl- and *n*-butanoyl 1,2-azir-

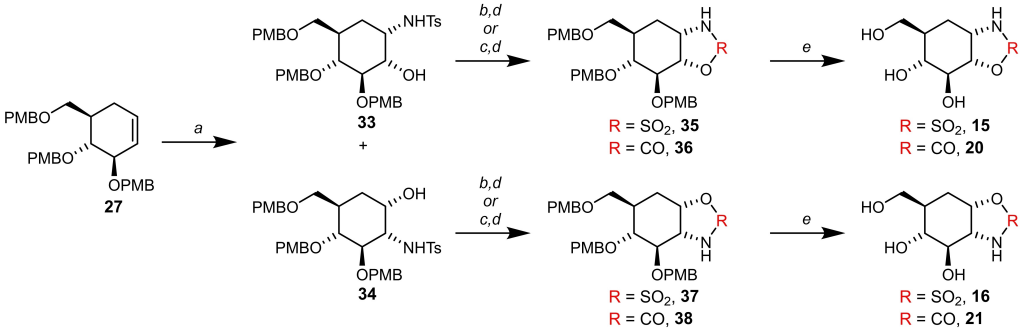

Scheme 3. Synthesis of cyclic sulfamidates **15** and **16**, and carbamates **20** and **21**. Reagents and conditions: (a) Chloramine-T, TEBACl, $K_2[OsO_2(OH)_4]$, 1:1 $CHCl_3$:H_2O, 18 h, 60 °C, 54% (**33**), 31% (**34**); (b) SO_2Cl_2, Et_3N, DCM, 2 h, −78 °C, quant. (**S4**), quant. (**S5**); (c) triphosgene, pyridine, DCM, 3 h, rt; (d) naphthalene, Na, THF, 30 min, −78 °C, 75% (**35**), 71% (**36**), 85% (**37**), 79% (**38**); (e) TFA, TES, DCM, 1 h, 0 °C, 94% (**15**), 67% (**20**), 81% (**16**), 32% (**21**).

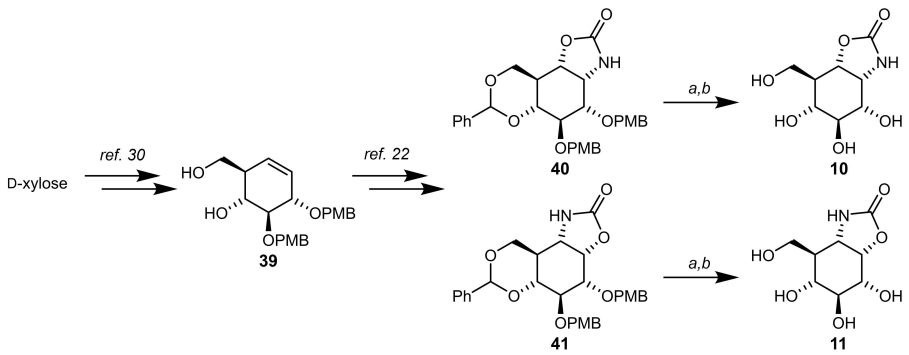

Scheme 4. Synthesis of cyclic carbamates **10** and **11**. Reagents and conditions: (a) *p*-TsOH, MeOH, 1 h, 40 °C (b) TFA, TES, DCM, 1 h, 0 °C, 74% (**10**), 86% (**11**).

Table 1. Apparent IC_{50} values for *in vitro* inhibition of rhGAA and ER-II.[a]

Compound	*In vitro* rhGAA IC_{50} (μM)	*In vitro* ER-II IC_{50} (μM)	Compound	*In vitro* rhGAA IC_{50} (μM)	*In vitro* ER-II IC_{50} (μM)
2	6.7 ± 0.34 [15 ± 2][b]	> 100 [> 100][b]	**12**	32.4 ± 4.6	11.3 ± 0.5
3	0.34 ± 0.091 [0.038 ± 0.003][b]	1.5 ± 0.08 [1.4 ± 0.1][b]	**13**	> 100	46.2 ± 2.6
4	0.060 ± 0.006 [0.082 ± 0.001][b]	0.029 ± 0.007 [0.029 ± 0.002][b]	**14**	2.63 ± 0.07	26.1 ± 3.2
5	6.1 ± 1.25 [5.17 ± 0.195][c]	> 100 [> 100][c]	**15**	> 100	> 100
6	20.2 ± 5.9 [112 ± 2.54][c]	1.03 ± 0.15 [47 ± 1.75][c]	**16**	> 100	> 100
7	1.96 ± 0.51	0.45 ± 0.03	**17**	> 100	> 100
8	0.84 ± 0.043	5.47 ± 0.91	**18**	> 100	> 100
9	> 100	> 100	**19**	> 100	> 100
10	12.5 ± 3.1	> 100	**20**	> 100	> 100
11	> 100	> 100	**21**	> 100	> 100

[a] All apparent IC_{50} values are determined from three technical triplicates. [b] Value in brackets contains literature reference data.[23] [c] Value in brackets contains literature reference data.[24]

idines **17** and **18** proved inactive as inhibitors of rhGAA and ER-II. Their 1,5a-analogues, compounds **7** and **8**, however, yielded micromolar rhGAA inhibitors. Slightly reduced inhibitory potency was observed for compound **7** and **8** (IC_{50} = 1.96 ± 0.51 μM and 0.84 ± 0.043 μM, respectively) in comparison to unfunctionalized aziridine **3**.

Turning to ER-II, compound **7** proved to be a 3-fold more potent inhibitor (IC_{50} = 0.45 ± 0.03 μM) whilst compound **8** showed a 3-fold reduction in inhibitory potency (IC_{50} = 5.47 ± 0.91 μM) compared to aziridine **3**. Cyclic sulfate **14** appeared to be a low-micromolar inhibitor of rhGAA (IC_{50} = 2.63 ± 0.07 μM), in contrast to its somewhat weaker inhibition of ER-II (IC_{50} = 26.1 ± 3.2 μM), giving compound **14** a roughly tenfold selectivity against rhGAA over ER-II. Its 1,5a-counterpart **4** proved to be a 100-fold more potent inhibitor of both rhGAA and ER-II (IC_{50} = 0.060 ± 0.006 μM and 0.029 ± 0.007 μM respectively).[23] Both the 1,2-cyclic sulfamidates **15** and **16** lacked the ability to reduce enzyme activities of both rhGAA as ER-II up to concentrations of 100 μM, demonstrating that migration of the sulfamidate from 1,5a to 1,2 does not lead to effective inhibitors. With regard to cyclic carbamates **10**, **11**, **20** and **21**, only compound **10** appeared to be an active inhibitor of rhGAA (IC_{50} = 12.5 ± 3.1 μM), which is in line with the structural relationship observed for the cyclic sulfamidates. In addition, inferior apparent IC_{50} values are observed for the 1,5a-(*N*,*O*)-regioisomers (**5** and **10**), which are roughly an order of magnitude more potent inhibitors when compared to the 1,5a-(*O*,*N*)-regioisomers (**6** and **11**). Finally, neither cyclic carbonates **9** nor **19** proved able to block rhGAA or ER-II activity.

Having identified the inhibitory potencies of compounds **2**–**21**, focus was shifted to determining the kinetic parameters and the mode of binding of some of the most active inhibitors on rhGAA. For this, rhGAA was incubated with a fixed substrate concentration and various inhibitor concentrations. Subsequently, apparent IC_{50} values were measured under varying incubation times. Compounds **2**, **3**, **4**, **6**, **7**, **8**, **12** and **14** showed a gradual decrease in enzyme activity indicating these compounds to be covalent and irreversible binders (Table 2). In

Table 2. Inhibitor kinetic constants for recombinant human α-glucosidase (rhGAA).[a]

Compound	Kinetic parameters in rhGAA k_{inact}/K_I (min^{-1} mM^{-1})	Mode of binding	Compound	Kinetic parameters in rhGAA k_{inact}/K_I (min^{-1} mM^{-1})	Mode of binding
2	0.1511 ± 0.0101 [0.37][b]	Covalent[b]	**12**	0.1526 ± 0.0102	Covalent
3	N.D. [58.0][b]	Covalent[b]	**13**	N.D.	N.D.
4	62.41 ± 3.82 [64.3][b]	Covalent[b]	**14**	1.389 ± 0.0592	Covalent
5	N.D.	Non-covalent[c]	**15**	N.D.	N.D.
6	0.06169 ± 0.0063 [0.7675][c]	Covalent[c]	**16**	N.D.	N.D.
7	N.D.	Covalent	**17**	N.D.	N.D.
8	N.D.	Covalent	**18**	N.D.	N.D.
9	N.D.	N.D.	**19**	N.D.	N.D.
10	N.D.	Non-covalent	**20**	N.D.	N.D.
11	N.D.	N.D.	**21**	N.D.	N.D.

[a] All apparent IC_{50} values are determined from two technical triplicates. [b] Value in brackets contains literature reference data.[23] [c] Value in brackets contains literature reference data.[24] N.D.: not determined.

contrast, both compound **5** and **10** appeared to be competitive inhibitors of rhGAA, as indicated by the observed lack of time dependency of the enzyme activity. Compounds **12** and **14** display pseudo first order kinetics due to fast inhibition against rhGAA, limiting measurement of a combined k_{inact}/K_I ratio.

Conformational free energy landscapes and target engagement. With the aim to obtain some more insight in the binding mode of the new 1,2-cyclophellitols, the gas-phase conformational free energy landscapes of the most potent 1,2-cyclophellitol inhibitors (**12**–**14**) were mapped next. Free energy landscapes (FELs) were computed by means of metadynamics simulations based on density functional theory (DFT, see Supporting Information).[37–47] For compounds **12** and **13**, the lowest energy conformation calculated is centred at $^4H_5$, with relative energies quickly inclining around this energy minimum (Figure 3B and D, respectively). This suggests compounds **12** and **13** to be relatively rigid and to mainly occupy this $^4H_5$ conformation. In contrast, their 1,5a-counterparts, **2** and **3**, exhibit local energy minima around the $^4H_3$ conformation, related to a 60° displacement along the ϕ-axis (Figure 3A, C, respectively). The lack of flexibility exhibited by compounds **12** and **13** prevents adoption of the $^4H_3$ conformation, required for suitable mimicry of the transition state.

The energy minimum of cyclic sulfate **14** is located around $^4C_1$, with a relatively wide minimum expanding toward the $^4H_3$-^4E-$^4H_5$ region, with even an additional energy minimum extending toward the $B_{3,0}$-$^1S_3$ region (Figure 3F). Again a 60° shift along the ϕ-axis is observed when compared to **4** (Figure 3E).[23] Interestingly, here an additional energy minimum is observed around the $B_{3,0}$-$^1S_3$ region not observed in parent structure **4**. These many low-energy conformations suggest **14** not only to adopt a $^4C_1$ conformation (mimicking the structure of the substrate at the Michaelis complex), but to be flexible enough to reach the $^4H_3$ transition state conformation. Thus, based on its conformational preferences, compound **14** should, as observed during *in vitro* assays, inhibit α-glucosidases with higher potencies in comparison to compounds **12** and **13**.

In order to ascertain whether the 1,2-cyclophellitol inhibitors binds to α-glucosidases of the CAZY GH31 family as predicted by the conformational analyses, the structure of **13** in complex with the model GH31 system Agd31B from *Cellvibrio japonicus* (a bacterial homologue of GAA) was determined at 1.9 Å resolution. **13** binds in the −1 subsite as expected (subsite nomenclature according to literature).[23,24,48] Serendipitously, as occasionally occurs with crystal soaks, the aziridine bound unopened in approximate $^1S_3/^4H_3$ conformation (Figure 4A). Asp412, the nucleophile, sits 3 Å "above" the atom equivalent to C1 of a glycoside with geometry poised for nucleophilic attack, and with Asp480, the acid/base, just 2.3 Å from the aziridine nitrogen. The structure confirms, "on enzyme", the conformational design of the 1,2-cyclophellitol as it lies in the low energy, favoured, region of the free energy landscape (Figure 3D).

Furthermore, we were struck by the shape of the 1,2-cyclophellitol design, in general, and the manner in which the shape and stereo/regiochemistry allows for substituents to lay astride the 1 and 2 positions tucked under below the sugar ring. Building on proposals that 1,2-cyclic phosphates could act as weak glycogen phosphorylase inhibitors,[49,50] we also wondered if 1,2-linked compounds would bind to *E. coli* maltodextrin phosphorylase, MalP, (a glycogen phosphorylase homolog).[51,52] Whilst we were unable to measure the binding constants for the compounds, soaking of crystals of MalP with **21** yielded a 1.9 Å structure which clearly showed binding in the catalytic centre (Figure 4B). suggesting that this scaffold may offer inspiration for future phosphorylase and glycosyltransferase inhibitor designs.

Discussion

This study reports on the preparation of a focused series of 1,2-*epi*-cyclophellitol analogues in comparison with their 1,5a-counterparts and their evaluation as inhibitors of recombinant human acid α-glucosidase (rhGAA) and ER α-glucosidase II (ER-II) and related enzymes. All 1,2-analogues (**12**–**21**) revealed reduced inhibitory potencies in comparison to their 1,5a-counterpart, with only compounds **12**–**14** exhibiting inhibitory potencies below 100 μM. The work presented here includes some 1,5a-*epi*-cyclophellitol derivatives with improved inhibition properties compared to what we reported previously. Of these, *N*-alkyl-1,5a-aziridine **7** inhibits ER-II more potently compared to its non-alkylated counterpart **3**, resulting in a nanomolar IC_{50} against ER-II with a 5-fold selectivity over rhGAA. Additionally, 1,5a-(*N*,*O*)-carbamate **10** revealed to be a non-covalent, low-micromolar inhibitor of rhGAA. Here, a strong structural relationship can be drawn with 1,5a-(*N*,*O*)-sulfamidate **5**, suggesting identical enzyme interactions are at play. Therefore, compound **10** may be an interesting candidate for further study as enzyme stabilizer that can be potentially used in treatment of Pompe disease. Conformational free energy landscapes revealed the ground state of compounds **12**–**14** to have undergone a shift in lowest energy conformation in comparison to their parent structures (**2**–**4**). As a result of this shift, the lowest energy conformation (approximated as $^4H_5$) neither resembles the conformation of the Michaelis complex nor the transition state during hydrolysis reflected by an energetic penalty for distortion to the conformation observed in crystal structures. This conformational shift may explain the overall reduction in observed inhibitory potencies of the 1,2-cyclophellitols in contrast to their 1,5a-counterparts. Although given the observed binding on maltodextrin phosphorylase, it is possible that the geometry of the compounds may inspire new inhibitor designs for transferases. In all, this study into structure-activity relationships of cyclophellitol analogues as human α-glucosidase inhibitors may fuel future design of constructs to effectively act on glycoside hydrolases of various sources and acting on various substrate glycosides.

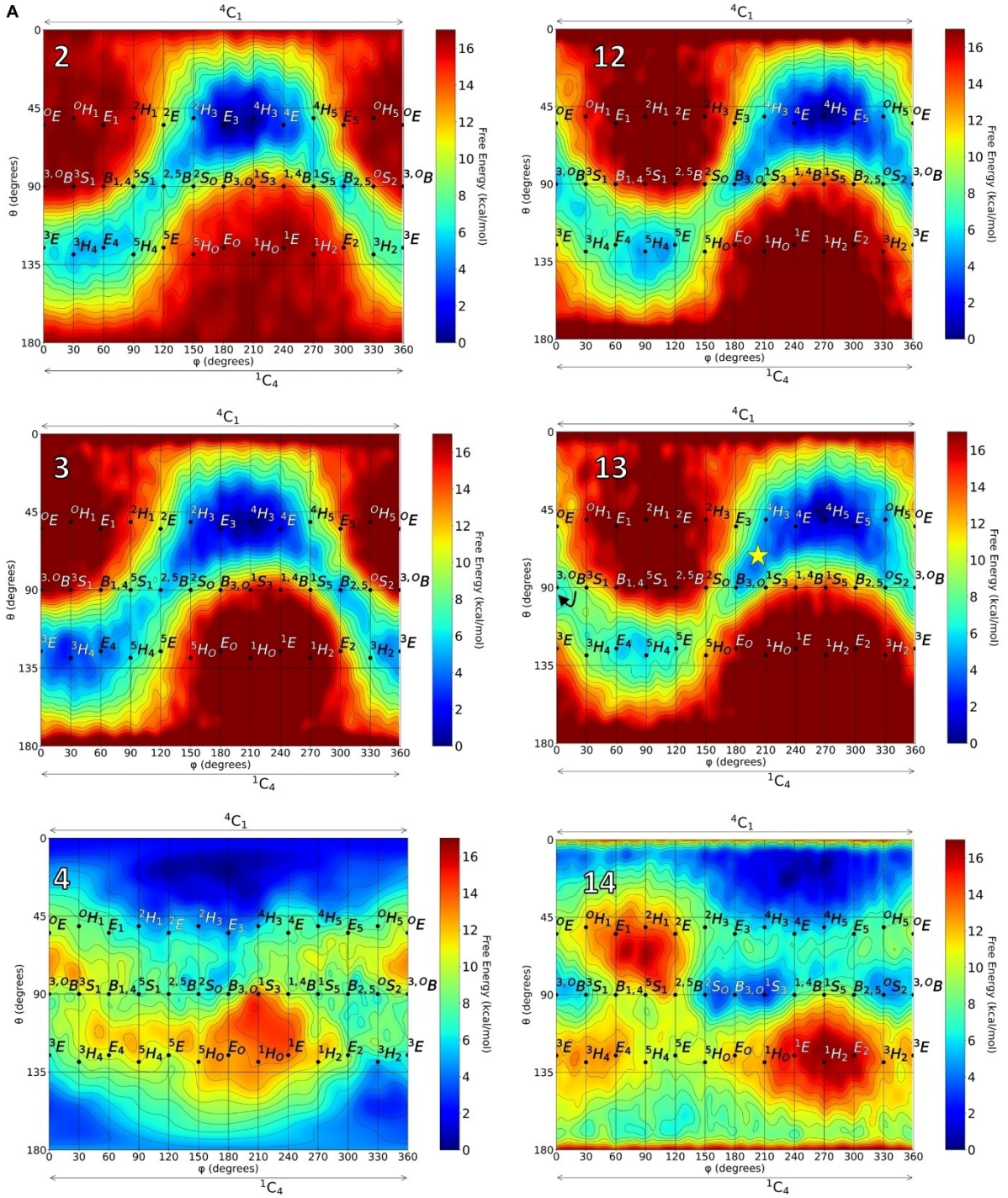

Figure 3. Gas-phase conformational free energy landscapes of (A) 1,5a-*epi*-cyclophellitol **2**, (B) 1,2-epoxide **12**, (C) 1,5a-aziridine **3**, (D) 1,2-aziridine **13** (E) cyclic 1,5a-sulfate **4** (adapted from Artola *et al.*[23]), and (F) cyclic 1,2-sulfate **14**. Isolines are 1 kcal/mol with the x and y axis representing the angle (in degrees) in Cremer-Pople puckering coordinates (ϕ and θ respectively). (D) The yellow star indicates the observed conformation of **13** in the −1 subsite of GH31 Agd31B from *Cellvibrio japonicus*. The arrow clarifies that label ^{3,O}B corresponds to the 0° point on the x axis and that all conformation labels appear on the right side of their corresponding points.

Experimental Section

Please find details on computational modelling, IC_{50} and kinetics determination, synthesis procedures, and experimental details in the Supporting Information.

Acknowledgements

This work was supported by the European Research Council (ERC-CoG-726072 "GLYCONTROL" to J.D.C.C. and ERC-2020-SyG-951231 "CARBOCENTRE" to H.S.O., C.R. and G.J.D.). GJD was

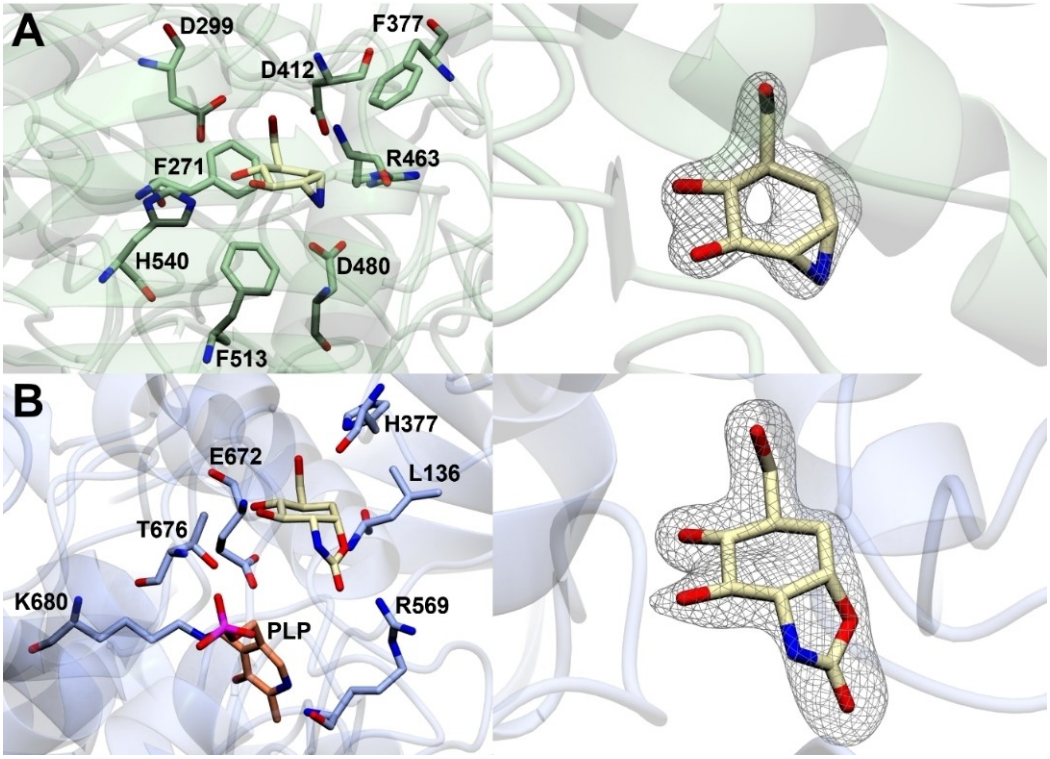

Figure 4. Comparison of the binding modes of 1,2-cyclophellitol based inhibitors towards glycoside hydrolases. All images were created and visualised in CCP4 mg (v. 2.10.11). All F_o-F_c maps (grey) have been displayed in chicken wire and contoured to 3.0 σ. A) Left hand panel: The active site of Agd31B, from *Cellvibrio japonicus*, in complex with one molecule of **13** (yellow). Active site residues (green) are labelled accordingly. Right hand panel: Omit density map for **13**. B) Left hand panel: The active site of MalP from *Escherichia coli*, in complex with one molecule of **21** (yellow). Active site residues (blue) and the PLP cofactor (orange) are labelled accordingly. Right hand panel: Omit density map for **21**.

supported by the Royal Society "Ken Murray" Research Professorship.We acknowledge Dr. Johan P. Turkenburg and Sam Hart for assistance with X-ray data collection; the staff of the Diamond Light Source (U.K.) for provision of i03 and i04 beamline facilities (proposal numbers mx32736 and mx24948). We thank Dr. Lluís Raich for technical assistance. The Viking cluster was used during this project, which is a high performance compute facility provided by the University of York. We are grateful for computational support from the University of York, IT Services and the Research IT team.

Conflict of Interests

The authors declare no conflict of interest.

Data Availability Statement

The data that support the findings of this study are available in the supplementary material of this article.

Keywords: Cyclophellitol · Glucosidase · Inhibitor · Conformational Analysis · Carbasugar

[1] L. L. Kiessling, R. A. Splain, *Annu. Rev. Biochem.* **2010**, *79*, 619–653.
[2] C. R. Bertozzi, L. L. Kiessling, *Science* **2001**, *291*, 2357–2364.
[3] R. A. Dwek, *Chem. Rev.* **1996**, *96*, 683–720.
[4] H. Ghazarian, B. Idoni, S. B. A. Oppenheimer, *Acta Histochem.* **2011**, *113*, 236–247.
[5] E. Drula, M. L. Garron, S. Dogan, V. Lombard, B. Henrissat, N. Terrapon, *Nucleic Acids Res.* **2022**, *50*, D571–D577.
[6] D. E. Koshland, *Proc. Natl. Acad. Sci. USA* **1958**, *44*, 98–104.
[7] A. Vasella, G. J. Davies, M. Böhm, *Curr. Opin. Chem. Biol.* **2002**, *6*, 619–629.
[8] D. L. Zechel, S. G. Withers, *Curr. Opin. Chem. Biol.* **2001**, *5*, 643–649.
[9] C. S. Rye, S. G. Withers, *Curr. Opin. Chem. Biol.* **2000**, *4*, 573–580.
[10] J. D. McCarter, S. G. Withers, *Curr. Opin. Struct. Biol.* **1994**, *4*, 885–892.
[11] G. Speciale, A. J. Thompson, G. J. Davies, S. J. Williams, *Curr. Opin. Struct. Biol.* **2014**, *28*, 1–13.
[12] S. Atsumi, H. Iinuma, H. Naganawa, H. Nakamura, T. Takeuchi, K. Umezawa, Y. Iitaka, *J. Antibiot.* **1990**, *43*, 49–53.
[13] T. K. M. Shing, Y. Cui, Y. Tang, *J. Chem. Soc. Chem. Commun.* **1991**, *11*, 756–757.
[14] K. Tatsuta, Y. Niwata, K. Umezawa, K. Toshima, M. Nakata, *J. Antibiot.* **1991**, *44*, 912–914.
[15] A. D. Mcnaught, H. B. F. Dixon, F. Cornish-Bowden, M. A. Chester, A. J. Barrett, J. C. Rigg, D. Horton, L. Anderson, D. C. Baker, H. H. Baer, J. N. Bemiller, B. Bossenbroek, R. W. Jeanloz, K. L. Loening, W. A. Szarek, R. S. Tipson, W. J. Whelan, R. L. Whistler, *Pure Appl. Chem.* **1996**, *68*, 1919–2008.
[16] R. E. McDevitt, B. A. Fraser-Reid, *J. Org. Chem.* **2002**, *59*, 3250–3252.
[17] S. P. Schröder, R. Petracca, H. Minnee, M. Artola, J. M. F. G. Aerts, J. D. C. Codée, G. A. van der Marel, H. S. Overkleeft, *Eur. J. Org. Chem.* **2016**, *28*, 4787–4794.
[18] C. De Boer, N. G. S. McGregor, E. Peterse, S. P. Schröder, B. I. Florea, J. Jiang, J. Reijngoud, A. F. J. Ram, G. P. Van Wezel, G. A. van der Marel, J. D. C. Codée, H. S. Overkleeft, G. J. Davies, *RSC Chem. Biol.* **2020**, *1*, 148–155.

[19] B. F. Cravatt, A. T. Wright, J. W. Kozarich, *Annu. Rev. Biochem.* **2008**, *77*, 383–414.
[20] S. P. Schröder, J. W. van de Sande, W. W. Kallemeijn, C.-L. Kuo, M. Artola, E. J. van Rooden, J. Jiang, T. J. M. Beenakker, B. I. Florea, W. A. Offen, G. J. Davies, A. J. Minnaard, J. M. F. G. Aerts, J. D. C. Codée, G. A. van der Marel, H. S. Overkleeft, *Chem. Commun.* **2017**, *53*, 12528–12531.
[21] L. I. Willems, H. S. Overkleeft, S. I. Van Kasteren, *Bioconjugate Chem.* **2014**, *25*, 1181–1191.
[22] J. Jiang, M. Artola, T. J. M. Beenakker, S. P. Schröder, R. Petracca, C. de Boer, J. M. F. G. Aerts, G. A. van der Marel, J. D. C. Codée, H. S. Overkleeft, *Eur. J. Org. Chem.* **2016**, *22*, 3671–3678.
[23] M. Artola, L. Wu, M. J. Ferraz, C.-L. Kuo, L. Raich, I. Z. Breen, W. A. Offen, J. D. C. C. Codée, G. A. van der Marel, C. Rovira, J. M. F. G. Aerts, G. J. Davies, H. S. Overkleeft, *ACS Cent. Sci.* **2017**, *3*, 784–793.
[24] K. Kok, C. L. Kuo, R. E. Katzy, L. T. Lelieveld, L. Wu, V. Roig-Zamboni, G. A. van der Marel, J. D. C. Codée, G. Sulzenbacher, G. J. Davies, H. S. Overkleeft, J. M. F. G. Aerts, M. Artola, *J. Am. Chem. Soc.* **2022**, *144*, 14819–14827.
[25] M. Alomari, M. Taha, F. Rahim, M. Selvaraj, N. Iqbal, S. Chigurupati, S. Hussain, N. Uddin, N. B. Almandil, M. Nawaz, R. Khalid Farooq, K. M. Khan, *Bioorg. Chem.* **2021**, *108*, 104638.
[26] F. Azimi, H. Azizian, M. Najafi, F. Hassanzadeh, H. Sadeghi-aliabadi, J. B. Ghasemi, M. Ali Faramarzi, S. Mojtabavi, Larijani, B. L. Saghaei, M. Mahdavi, *Bioorg. Chem.* **2021**, *114*, 105127.
[27] S. P. Schröder, L. Wu, M. Artola, T. Hansen, W. A. Offen, M. J. Ferraz, K.-Y. Li, J. M. F. G. Aerts, G. A. van der Marel, J. D. C. Codée, G. J. Davies, H. S. Overkleeft, *J. Am. Chem. Soc.* **2018**, *140*, 5045–5048.
[28] I. Frau, V. Di Bussolo, L. Favero, M. Pineschi, P. Crotti, *Chirality* **2011**, *23*, 820–826.
[29] A. V. R. L. Sudha, M. Nagarajan, *Chem. Commun.* **1998**, *3*, 31.
[30] V. W.-F. Tai, P. H. Fung, Y. S. Wong, T. K. M. Shing, *Tetrahedron: Asymmetry* **1994**, *5*, 1353–1362.
[31] D. Lu, S. Zhu, L. F. Sobala, G. Bernardo-Seisdedos, O. Millet, Y. Zhang, J. Jiménez-Barbero, G. J. Davies, M. Sollogoub, *Org. Lett.* **2018**, *20*, 7488–7492.
[32] M. Artola, S. Wouters, S. P. Schröder, C. de Boer, Y. Chen, R. Petracca, A. M. C. H. van den Nieuwendijk, J. M. F. G. Aerts, G. A. van der Marel, J. D. C. Codée, H. S. Overkleeft, *Eur. J. Org. Chem.* **2019**, *6*, 1397–1404.
[33] H. Tsunoda, S. Ogawa, *Liebigs Ann.* **1995**, *2*, 267–277.
[34] F. G. Hansen, E. Bundgaard, R. Madsen, *J. Org. Chem.* **2005**, *70*, 10139–10142.
[35] G. Luchetti, K. Ding, M. D'Alarcao, A. Kornienko, *Synthesis* **2008**, *19*, 3142–3147.
[36] B. Lacourt-Gadras, M. Grignon-Dubois, B. Rezzonico, *Carbohydr. Res.* **1992**, *235*, 281–288.
[37] R. Car, M. Parrinello, *Phys. Rev. Lett.* **1985**, *55*, 2471–2474.
[38] P. Hohenberg, W. Kohn, *Phys. Rev. Lett.* **1964**, *136*, B864.
[39] W. Kohn, *Phys. Rev. A* **1965**, *1133*, 140–148.
[40] CPMD V3.9 Copyright IBM Corp 1990–2004, Copyright MPI für Festkörperforschung Stuttgart 1997–2001.
[41] J. P. Perdew, K. Burke, M. Ernzerhof, *Phys. Rev. Lett.* **1996**, *77*, 3865–3868.
[42] A. Ardèvol, C. Rovira, *J. Am. Chem. Soc.* **2015**, *137*, 7528–7547.
[43] M. Marianski, A. Supady, T. Ingram, M. Schneider, C. Baldauf, *J. Chem. Theory Comput.* **2016**, *12*, 6157–6168.
[44] N. Troullier, J. L. Martins, *Phys. Rev. B* **1991**, *43*, 1993–2006.
[45] A. Laio, M. Parrinello, *Proc. Natl. Acad. Sci. USA* **2002**, *99*, 12562–12566.
[46] G. A. Tribello, M. Bonomi, D. Branduardi, C. Camilloni, G. Bussi, *Comput. Phys. Commun.* **2014**, *185*, 604–613.
[47] P. Tiwary, M. Parrinello, *J. Phys. Chem. B* **2015**, *119*, 736–742.
[48] J. Larsbrink, A. Izumi, G. R. Hemsworth, G. J. Davies, H. Brumer, *J. Biochem.* **2012**, *287*, 43288–43299.
[49] F. C. Kokesh, R. K. Stephenson, Y. Kakuda, *Biochim. Biophys. Acta* **1977**, *483*, 258–262.
[50] H. Y. Hu, M. Allen, *Biochim. Biophys. Acta* **1978**, *525*, 55–60.
[51] M. O'Reilly, K. A. Watson, R. Schinzel, D. Palm, L. N. Johnson, *Nature Struc. Bio.* **1997**, *4*, 405–412.
[52] S. Geremia, M. Campagnolo, R. Schinzel, L. N. Johnson, *J. Mol. Biol.* **2002**, *322*, 413–423.

Manuscript received: February 22, 2024
Accepted manuscript online: April 16, 2024
Version of record online: ■■, ■■

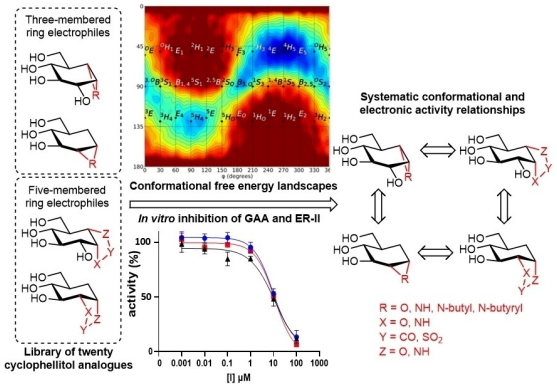

Twenty configurational and functional cyclophellitol analogues were synthesized and evaluated on their potency as retaining α-glucosidase inhibitors. The inhibitory properties of the focused library of compounds were determined on human α-glucosidases after which we mapped the conformational free energy landscapes of the most active compounds. Our results add to the growing list of covalent and competitive α-glucosidase inhibitors and may pave the way towards the design of new therapeutics targeting these enzymes.

*Dr. T. P. Ofman, J. J. A. Heming, Dr. A. Nin-Hill, Dr. F. Küllmer, E. Moran, M. Bennett, R. Steneker, A.-M. Klein, G. Ruijgrok, K. Kok, Dr. Z. W. B. Armstrong, Prof. Dr. J. M. F. G. Aerts, Prof. Dr. G. A. van der Marel, Prof. Dr. C. Rovira, Prof. Dr. G. J. Davies, Dr. M. Artola, Prof. Dr. J. D. C. Codée, Prof. Dr. H. S. Overkleeft**

1 – 10

Conformational and Electronic Variations in 1,2- and 1,5a-Cyclophellitols and their Impact on Retaining α-Glucosidase Inhibition